Electrochimica Acta 86 (2012) 177–184

Contents lists available at SciVerse ScienceDirect

Electrochimica Acta

journal homepage: www.elsevier.com/locate/electacta

Electrokinetic-enhanced nanoscale iron reactive barrier of trichloroethylene solubilized by Triton X-100 from groundwater

Yi-Chu Huang*, Ya-Wen Cheng

Department of Environmental Science and Engineering, National Pingtung University of Science and Technology, 1 Hseuh Fu RD., Nei Pu Township, Pingtung 91201, Taiwan

ARTICLE INFO

Article history:
Received 21 October 2011
Received in revised form 10 March 2012
Accepted 12 March 2012
Available online 19 March 2012

Keywords:
Electrolysis
Surfactant
Permeable reactive barrier
Chlorinated solvents
Sandbox

ABSTRACT

The objective of this study is to investigate the performances of permeable reactive barrier (PRB) packed with nanoscale zero-valent iron (NZVI) particles enhanced by surfactant and electrokinetics (EK) on trichloroethylene (TCE) degradation. The optimal operation parameters obtained from the tests conducted in a lab-scale sandbox were the potential gradient of 1 V cm^{-1}, NZVI loading of 5 g, and PRB located behind the anode, and were adopted for the following transport and degradation experiments conducted in the bench-scale sandbox. Chlorinated byproducts were not detected during the lab-scale sandbox tests, i.e. TCE was completely dechlorinated by NZVI particles in the reactive barrier. The results of bench-scale sandbox tests revealed that TX100 surfactant raised the mobility and solubility of TCE in aquifer that increased its availability for further dechlorination of NZVI. Advection and dispersion were the main factors on reduction of TX100 while adsorption of sand had higher influences on the decrease of TCE. The concentrations of TCE in the lower layer are higher than those in the upper layer owing to its dense non-aqueous phase liquid (DNAPL) properties. EK can promote the reactivity of NZVI by releasing H^+ near anode. H^+ not only participates in TCE dechlorination reaction but also washes away the precipitates on surface of NZVI to maintain its activity. Fe^{2+} and Cl^- were continuously produced accompanying with TCE degradation showing that TCE was dechlorinated by NZVI particles. This study shows that NZVI coupling with EK can promote the degradation of TCE in groundwater.

1. Introduction

Chlorinated solvents such as trichloroethylene (TCE) and tetrachloroethylene (PCE) identified in many contaminated sites are not readily degraded or decomposed in the environment owing to their characteristics of dense non-aqueous phase liquids (DNPALs). Some of those solvents have been recognized as carcinogens and toxins to human being because of their toxicity and bioaccumulation. Therefore, there is an urgent need to develop effective control and treatment methods to remediate the aquifers contaminated by chlorinated solvents.

So far, some technologies for removing chlorinated contaminants from aquifer were proposed such as pump-and-treat, air sparging coupling with vapor extraction, permeable reactive barrier (PRB), electrokinetics (EK), oxidation and reduction with reagents, thermal treatment, and bioremediation. Remediation practices in the past indicated that each of those remediation methods demonstrated its pro effects under certain environmental conditions, but con results under other conditions. The remediation aims of contaminated groundwater are to mineralize pollutants in situ or to remove them from aquifer and further to treat ex situ, or to confine their transport within porous media. Generally speaking, in situ remediation methods demonstrate more advantages than pump-and-treat technology. PRB, a passive in situ remediation approach, possesses additional benefits of not requiring any energy consumption, less labor-intensive, and operation safety [1–6].

Among the remediation technologies, zero-valent iron (ZVI) has been shown effective for the reductive dechlorination of the chlorinated contaminants in groundwater [7–12]. The major reductants in the Fe^0–H_2O system were Fe^0, Fe^{2+}, and H_2 released from iron corrosion and Fe^0 was the dominant reductant for dechlorination of carbon tetrachloride [7]. Generally, the reductive dechlorination of chlorinated compounds by Fe^0 occurs with two electrons transferred from Fe^0 to contaminants according to Eq. (1) [13–15].

$$Fe^0 + RCl + H^+ \rightarrow Fe^{2+} + RH + Cl^- \quad (1)$$

Reduction of chlorinated compounds by iron is launched via two pathways: hydrogenolysis, a Cl^- replaced by a hydride ion, and reductive β-elimination, two Cl^- released. Both of the pathways are accompanied by a net exchange of two electrons [7,16,17]. However, several defects of the ZVI technique limited its practical application. First, once ZVI is exposed to air or contact with the reactants in aqueous solution, its reaction activity quickly

* Corresponding author. Tel.: +886 8 7703202x7379; fax: +886 8 7740406.
E-mail addresses: ych@mail.npust.edu.tw, ych6802.ych6802@msa.hinet.net (Y.-C. Huang).

0013-4686/$ – see front matter © 2012 Elsevier Ltd. All rights reserved.
doi:10.1016/j.electacta.2012.03.048

decreased because an oxide layer is liable to form on the surface of Fe^0 [3,9,10]. Second, some of the lightly chlorinated byproducts, which may be more toxic, produced by the dechlorination of parent contaminants accumulate in ZVI remediation system, and cannot be further degraded [8,13]. Vinyl chloride (VC), more toxic than its parent compounds, was produced and accumulated at the end of their batch and column tests for degradation of 1,1,2-TCA (trichloroethane) and TCE with ZVI [11].

Therefore, many methods focused on the improvement of ZVI reactivity have been developed. First, the size of ZVI particles can be nanoized to increase the reaction rates and further enhance the degradation of chlorinated solvents in water [18–22]. PCE in water could be rapidly and completely dechlorinated by nanoscale ZVI (NZVI), but only a small amount of PCE was degraded with microscale ZVI [13]. Second, EK integrated with PRB packed with ZVI has been shown as an effective and safe method to remediate the aquifer contaminated by chlorinated solvents [23–27]. Actually, EK technologies are gaining more and more respect for remediation of aquifer contaminated with metals and organic compounds [28–30]. EK plays the role of an H^+ provider that is produced from water electrolysis in accordance with Eqs. (2) and (3) [13]. The results of integration of ZVI with EK for remediation of soils contaminated by PCE showed that 99% and 90% of PCE in the pore water and soil were removed, respectively, after a 10-day treatment [13].

$$\text{Anode}: \quad 2H_2O \rightarrow O_{2(g)} + 4H^+ + 4e^- \tag{2}$$

$$\text{Cathode}: \quad 2H_2O + 2e^- \rightarrow H_{2(g)} + 2OH^- \tag{3}$$

Surfactant-enhanced aquifer remediation (SEAR) has been demonstrated as a favorable technology to promote the solubility and mobility of hydrophobic pollutants in aquifer with application of surfactants [31–37]. Solubilization and mobilization of those hydrophobic pollutants within porous medium are achieved by the micelles formation and emulsification effect of surfactants. Based on the pseudo-first order reaction rate law, the presence of 1 critical micelle concentration (cmc) of sodium dodecyl sulfate (SDS) increased the reaction rate by a factor of 2.5 when the NZVI was used for degrading TCE in a water solution. SDS was effective for enhancing degradation of TCE sorbed in soil, the presence of SDS at sub-cmc increased TCE degradation rate by ~10% [38]. Anionic and nonionic surfactants might inhibit the reductive dechlorination of TCE because of the decrease of TCE sorption on the surface of ZVI [15]. However, surfactant can enhance the mobility of TCE within the aquifer that increases the availability of TCE for degradation by NZVI PRB [5]. Moreover, nonionic surfactants are less toxic than cationic and anionic surfactants.

The objective of this study is to investigate the performances of PRB packed with NZVI enhanced by surfactant and EK on TCE degradation. Experiments were performed in two stages. Tests of the first stage were conducted in a lab-scale sand box to determine the optimal parameters such as potential, iron barrier site, and iron amounts of electro-enhanced NZVI PRB (ENZVIPRB) on TCE degradation. Tests of the second stage were carried out with the above-mentioned optimal parameters in a bench-scale sand box to study the solute transport through porous media and the effects on TCE degradation. The results of this study may provide some useful information for application of NZVI PRB system on remediation of aquifers contaminated by chlorinated solvents.

2. Experimental

2.1. Chemicals

All chemicals were reagent grade and used as received. TX100 (alkalaryl polyether alcohol ($C_{14}H_{22}O(C_2H_4O)_n$), Triton X-100, molecular weight = 625 g mol^{-1}) and TCE (C_2HCl_3, 99.9%, HPLC grade) were obtained from J.T. Baker. The reported values of hydrophile–lipophile balance and critical micellar concentration of TX100, a non-ionic surfactant, are 13.9 and 140 mg L^{-1}, respectively. Methanol (CH_3OH, HPLC grade) was purchased from Merck. Sodium borohydride ($NaBH_4$, 99.5%) and ferric chloride ($FeCl_3{\cdot}6H_2O$, 99.5%) were purchased from Alfa Aesar.

2.2. NZVI preparation

NZVI particles were synthesized by mixing 1:1 volume ratio of 0.50 M $NaBH_4$ with 0.28 M $FeSO_4{\cdot}7H_2O$ under intensive agitation. NZVI particles formed according to the Eq. (4) were filtered out, rinsed with Milli-Q deionized water, and dried via a freeze dryer (Eyela FDU-1200) for 24 h. The preparation process must be quick and continuous to keep the NZVI fresh. After the drying processes, the NZVI particles in the brown bottle were filled with nitrogen gas and sealed to prevent them from further oxidation.

$$2Fe^{2+}{}_{(aq)} + BH_4{}^-{}_{(aq)} + 3H_2O_{(l)} \rightarrow 2Fe^0{}_{(s)} + H_2BO_3{}^-{}_{(aq)} + 4H^+{}_{(aq)} + 2H_{2(g)} \tag{4}$$

2.3. Particle characterization

Particle sizes of prepared NZVI were determined by a laser particle diameter analyzer (Beckman Coulter N5), and the BET specific surface area was measured by a surface area analyzer (Beckman Coulter SA3100) using the nitrogen adsorption method at 77 K. The average particle diameter and specific surface area of the lab-synthesized iron particles were 79 nm and 30 m^2 g^{-1}, respectively. The surface morphology and contents of test particles were observed through a scanning electronic microscopy (SEM) equipped with an energy dispersive spectrometer (EDS) (Hitachi S-3000N). SEM images observed at beam energies of 10 kV and magnification of 50,000 times showed the surface of NZVI particles was chain-like and rough. The results of SEM–EDS analysis indicated that Fe was the major element on the surface of particles. Fe component of prepared particles was also verified via X-ray powder diffraction (XRD) (Rikagu Rint2000) at $2\theta = 44.74^\circ$. The functional groups on the surface of NZVI after TCE reduction were observed via a Fourier transform infrared spectrometer (FTIR) (Bruker Vector 22).

2.4. Analysis methods

TCE, 1,1-DCE, cis-1,2-DCE, trans-1,2-DCE, VC, and TX100 were detected by a HPLC (Hitachi L-7100) equipped with a Mightsil RP-18 column and a UV–vis detector (Hitachi L-7420). The UV wavelength for TCE and TX100 detection was set at 240 nm, and at 210 nm for 1,1-DCE, cis-1,2-DCE, trans-1,2-DCE and VC. The mobile phase for TCE and TX100 was 80% methanol and 20% water (v/v), and 75% methanol and 25% water (v/v) for other compounds. The flow rate was set at 1.5 mL min^{-1} for TCE and TX100, and 1.0 mL min^{-1} for other compounds. Cl^- was detected by an ion chromatography (Dionex-120) equipped with a Dionex AS-12A column. The flow rate of the mobile phase containing 2.7 mM Na_2CO_3 and 0.3 mM $NaHCO_3$ was kept at 1.5 mL min^{-1}. Fe^{2+} was measured by a UV–vis spectrophotometer (Hach-DR 2400).

2.5. Sandbox experiments

A lab-scale sandbox (not shown) made of glass with 20 cm length, 5 cm width, and 5 cm height was designed to determine the optimal parameters such as potential, site of iron barrier, and iron amounts of EK-enhanced NZVI PRB on TCE degradation, while a bench-scale glass sandbox with 40 cm length, 5 cm width, and

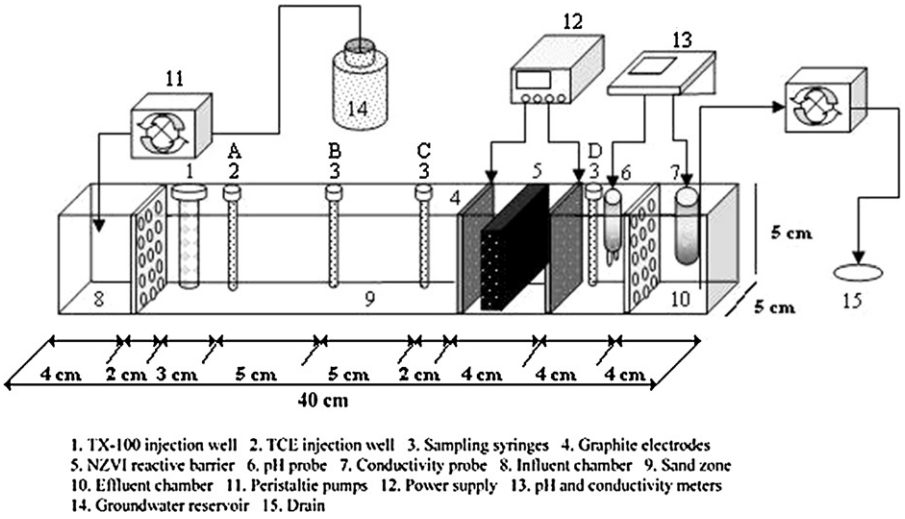

Fig. 1. Schematic diagram of the sandbox for transport and degradation experiments.

5 cm height was devised to simulate the transport and degradation of TCE in aquifer (Fig. 1). The middle zone of both the lab-scale and bench-scale sandbox was filled with silica sand and was divided from the left and right chambers with perforated acrylic boards and steel sieves (0.25 mm mesh). Two chambers with dimensions of 4 cm × 5 cm × 5 cm (length × width × height) were used as reservoirs to stabilize the water flowing through the sand zone by controlling the water level between the two chambers with peristaltic pump. The 2-cm wide PRB was separated from the sand zone with two perforated acrylic boards, glass-fiber filter (1.5 μm pore size), and steel sieves (0.25 mm mesh). Both the lab-scale and bench-scale sandboxes were sealed up with a cover to avoid escaping of TCE. The height and width of silica sand within sandbox was about 4.5 cm and 5 cm, respectively. The porosity of silica sand with particle sizes of 0.25–0.5 mm was 0.394 ± 0.02.

For the lab-scale sandbox, groundwater was continuously circulated at around 60 mL h^{-1} from effluent chamber back into influent chamber by a small-scale peristaltic pump. The locations of anodic and cathodic graphite electrodes were 0 and 10 cm away from the influent chamber. Concentrations of TCE, TX100, and Fe^{2+}, as well as electric current and pH were periodically monitored behind PRB and in the effluent chamber.

Because of the various cross-section area between the lab- and bench-scale sandbox, groundwater was continuously supplied from a reservoir at about 24 mL h^{-1} to the left chamber and continuously moved through the sand zone and then drained from the right chamber with the same flow rate for the bench-scale sandbox. Average flow speed of groundwater in the sand zone was around 3.05 cm h^{-1}. The properties of silica sand and groundwater were also analyzed. Two transport and two degradation experiments were conducted. The experiments conducted were designed to simulate the transport behaviors of TX100, the effect of TX100 on TCE solubility enhancement, TCE degradation with NZVI PRB and EK, and TX100 enhanced TCE degradation with NZVI PRB and EK. The operational parameters of transport and degradation tests are shown in Table 1.

2.5.1. TX100 and TCE Transport

The influent and effluent rates of groundwater were first adjusted to achieve dynamic equilibrium and maintain the water level of both chambers at a height of 3.5 cm, then 50 mL of 1400 mg L^{-1} TX100 solution was added into injection well with a peristaltic pump at 50 mL h^{-1}. TX100 concentrations in the lower layer of sandbox were periodically collected at sampling points of A1, B1, and C1 located in the sand zone. The distance from injection well to points A1, B1, and C1 was 3, 13, and 26 cm, respectively (not shown in Fig. 1). Tests of TX100-enhanced TCE transport were also conducted following the similar steps. As the groundwater flow attained the steady state, 0.5 mL pure TCE was injected to the bottom of point A (Fig. 1). After 24 h, 50 mL of 1400 mg L^{-1} TX100 solution was added into injection well with a peristaltic pump at 50 mL h^{-1}. TCE and TX100 concentrations in the lower layer of sandbox were also periodically monitored at sampling points of A, B, C, and D located in the sand zone. The distance from injection well to points A, B, C, and D was 3, 8, 18, and 26 cm, respectively (Fig. 1).

2.5.2. TCE degradation with NZVI reactive barrier and EK

When the groundwater flow in the sand zone achieved steady state, 5 mL of pure TCE was added into the lower layer of point A. After 22 h, 5 g NZVI was put into the PRB to degrade the TCE in water. The 4-cm wide PRB was placed between points C and D, and separated from the sand zone with two perforated acrylic boards, glass-fiber filter (1.5 μm pore size), and steel sieves (0.25 mm mesh). After 54 h of operation, KCl (0.01 N) was injected into sandbox as electrolytes and waited 28 h more to reach stable condition for the following operation of EK. Moreover, anodic and cathodic graphite electrodes were placed in front and rear of PRB respectively, and connected to the direct-current power supply at the 84th hour. The potential gradient was maintained at 1 V cm^{-1}. Concentrations of residual TCE and its potential chlorinated byproducts including 1,1-DCE, cis-1,2-DCE, trans-1,2-DCE and VC were periodically monitored in the upper (3 cm above the bottom of sandbox) and lower layers (1 cm) at points A, B, C, and D. Cl^- released from the TCE dechlorination was also measured.

2.5.3. TX100-enhanced TCE degradation with NZVI reactive barrier and EK

Continuing with the test performed in Section 2.5.2, 50 mL of 1400 mg L^{-1} TX100 was added into aquifer through the injection well to enhance the mobility of TCE at the 112nd hour. After 142 h of operation, another 50 mL of 1400 mg L^{-1} TX100 was added. TX100 and TCE as well as its potential degradation byproducts in the upper (3.5 cm above the bottom of sandbox), mid (2 cm), and (0.5 cm) layers of sandbox were also periodically monitored at sampling points of B, C, and D.

Table 1
Operational parameters of transport and degradation tests in a bench-scale sandbox.

Tests	NZVI (g)	TX100 concentration ($mg\,L^{-1}$)	Voltage gradient ($V\,cm^{-1}$)	Q^a ($mL\,h^{-1}$)	U^b ($cm\,h^{-1}$)	HRT[c] (h)
TX100 transport	–	1400	–	24	3.05	8.5
TX100-enhanced TCE transport	–	1400	–	24	3.05	8.4
TCE degradation with NZVI	5	–	–	24	3.05	8.5
TCE degradation with NZVI and EK	5	–	1	24	3.05	8.5
TX100-enhanced TCE degradation with NZVI and EK	5	1400	1	24	3.05	8.5

[a] Q: flow rate of groundwater in sand zone.
[b] U: average flow speed of groundwater in sand zone.
[c] HRT: theoretical hydraulic residence time from injection well to point D.

3. Results and discussion

3.1. Optimal operation tests in a lab-scale sandbox

For test 1 shown in Table 2, only 1.4% of TCE lost in a closed system which showed that the degradation and evaporation rates of TCE were insignificant after 14 h of operation. Besides, addition of electrolyte and application of potential had little effect on TCE degradation (test 2). As shown in tests 3–6, the higher the potential gradient applied, the greater the TCE removal rates were. The primary reasons may be that the passive layer of NZVI particles was washed away by the H^+ released by electrolysis of water and TCE received the electrons released near anode to accomplish its reductive dechlorination process. TCE removal efficiency of potential gradient set at $0.5\,V\,cm^{-1}$ was approximately the same as that with addition of 5 g of NZVI, i.e. without applying EK. As the potential gradient increased to 1 and $2\,V\,cm^{-1}$, TCE removal ratios at the outlet of sand box could reach to 95.2% after 14 h and 96.6% after 8 h of operation, respectively. Although TCE removal efficiency increased with higher potential gradient, some precipitates deposited on the iron surface could block the pores of PRB as potential gradient set at $2\,V\,cm^{-1}$ was not suitable for a long-term operation. As observed in tests 5 and 9, although the variation of NZVI loading was only 2 g, TCE removal rate significantly increased from 36% to 95%. TCE removal rate per gram of NZVI loading was enhanced due to the small particle sizes and high specific surface area of NZVI. From the results of tests 5, 7, and 8, TCE removal rates for PRB behind the anode were higher than those for PRB near the cathode or located in the middle of sandbox because of the release of H^+ and electrons behind the anode by application of electric potentials. Chlorinated by-products, including 1,1-DCE, cis-1,2-DCE, trans-1,2-DCE, and VC, were not detected at the sampling point behind the PRB. Furthermore, TX100 was not degraded by NZVI (test 10). Concentrations of Fe^{2+} monitored increased with higher NZVI loadings and potential gradients. As shown in Table 2, application of NZVI and potential lowered the pH in solution behind the anode but raised it near the cathode. Therefore, the optimal operation parameters could be determined as the potential gradient of $1\,V\,cm^{-1}$, NZVI loading of 5 g, and PRB located behind the anode, and were adopted for the following transport and degradation experiments conducted in the bench-scale sandbox.

3.2. Transport tests in a bench-scale sandbox

Fig. 2a displays the variations of TX100 concentrations at three sampling points along the transport test. TX100 was first observed at point C1 at the 9th hour close to the theoretical hydraulic residence time (HRT) of 8.5 h (26 cm/3.05 $cm\,h^{-1}$) from the injection well to point C1. The breakthrough time of TX100 was slightly slower than that of water flow which implied that it was not significantly degraded and dispersed during the transport in aquifer as well as not readily adsorbed by the silica sand. The concentration curves in Figs. 2a, 3a and b reveal a tendency to change from the sharp to flat shape with transport distance. This phenomenon resulted mainly from the effects of advection, dispersion, adsorption, and chemical/biological reaction within the aquifer. Generally speaking, the area under concentration curves as shown in Fig. 2b should be the same provided that the transport of solutes through porous medium is affected only by advection and dispersion. Otherwise it is also affected by adsorption and chemical/biological reactions. The details to quantify the influence proportion of advection, dispersion, adsorption, and chemical/biological reactions of the solutes transporting through the porous medium can be found in the literatures [39–41]. The highest four concentrations sampled at points A1, B1, and C1 were selected to compute their average concentrations (C) and the average one at point A1 was treated as the initial concentration (C_0). Besides, the area (A) under the concentration curves was calculated to represent the solute quantity per unit flow rate that passes through respective point and the area of point

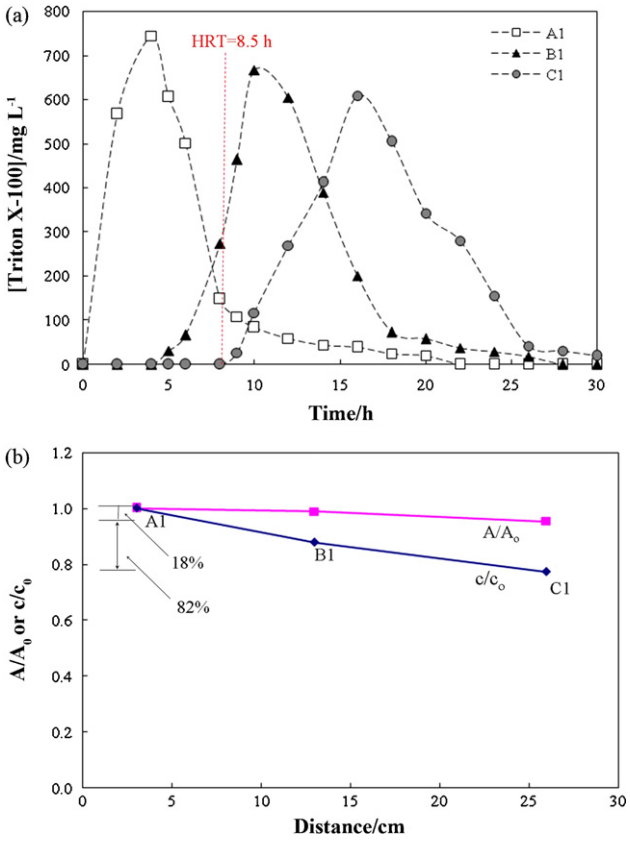

Fig. 2. (a) Variations of TX100 concentrations and (b) relationship between residual TX100 (area under the concentration curve) and transport distance along the transport test of 1400 $mg\,L^{-1}$ TX100.

Table 2
Operational parameters and performance for the tests of TCE and TX100 degraded by NZVI particles enhanced by EK in a lab-scale sandbox.

Test[a]	NZVI (g)	Potential gradient (V cm^{-1})	Initial PCE conc. (mg L^{-1})	TX100 conc. (mg L^{-1})	Final PCE conc. (mg L^{-1})	PCE removal (%)	PRB location	Initial pH	Final pH
1	0	0	50	0	49.3	1.4	–	6.6	7.1
2	0	1	50	0	45.2	9.6	–	6.6	3.9(9.4)[c]
3	5	0	50	0	23.2	53.6	Middle	6.7	9.4
4	5	0.5	50	0	21.1	57.8	Middle	7.2	7.0(9.5)
5	5	1	50	0	2.4	95.2	Middle	6.7	3.8(10.1)
6	5	2	50	0	1.7	96.6	Middle	6.8	3.0(11.3)
7	5	1	50	0	1.1	97.8	Behind anode	7.1	9.6
8	5	1	50	0	12.0	76.0	Near cathode	7.2	3.2(9.8)
9	3	1	50	–	32.2	35.5	Middle	7.0	4.5(8.6)
10	5	1	–	1400(1354)[b]	–	–	Middle	6.7	9.4

[a] Operation time was 8 h for test 6, 10 h for test 7, and 14 h for tests 1–5 and 8–10.
[b] Initial and final concentrations of TX100 were 1400 and 1354 mg L^{-1}, respectively.
[c] Final pH behind anode (final pH near cathode) as EK was applied.

A1 was also treated as the initial quantity per unit flow rate (A_0). As shown in Fig. 2b, the values of C/C_0 and A/A_0 decreased around 5% and 23% from point A1 to C1, respectively. Therefore the proportion for the effects of adsorption and biological/chemical factors on TX100 reduction was estimated to be 18% and 82% for advection and dispersion.

As shown in Fig. 3a, TCE concentration ranged between 250 and 270 mg L^{-1} at various sampling points in the absence of TX100 while increased to 700 mg L^{-1} with addition of 50 mL of 1400 mg L^{-1} TX100. The results indicated that the solubility and mobility of TCE obviously enhanced about 2.6 times in the presence of TX100. Besides, TX100 concentrations detected were around 700 mg L^{-1} for points B, C, and D at the respective operation time of 27, 33, and 37 h (Fig. 3b). Fig. 3c presents that the proportions of 29% and 71% were obtained for the effects of adsorption/biological/chemical and advection/dispersion factors on TCE reduction, respectively. The high proportion of adsorption/biological/chemical effects may be due to the hydrophobic properties of TCE which is readily adsorbed by the silica sand and the slight degradation moving through the sand zone. As for TX100 reduction, Fig. 3d shows that the proportion of adsorption and biological/chemical effects was estimated to be 12% and 88% for advection and dispersion. As shown in Figs. 2b and 3d, the proportion of factors for TX100

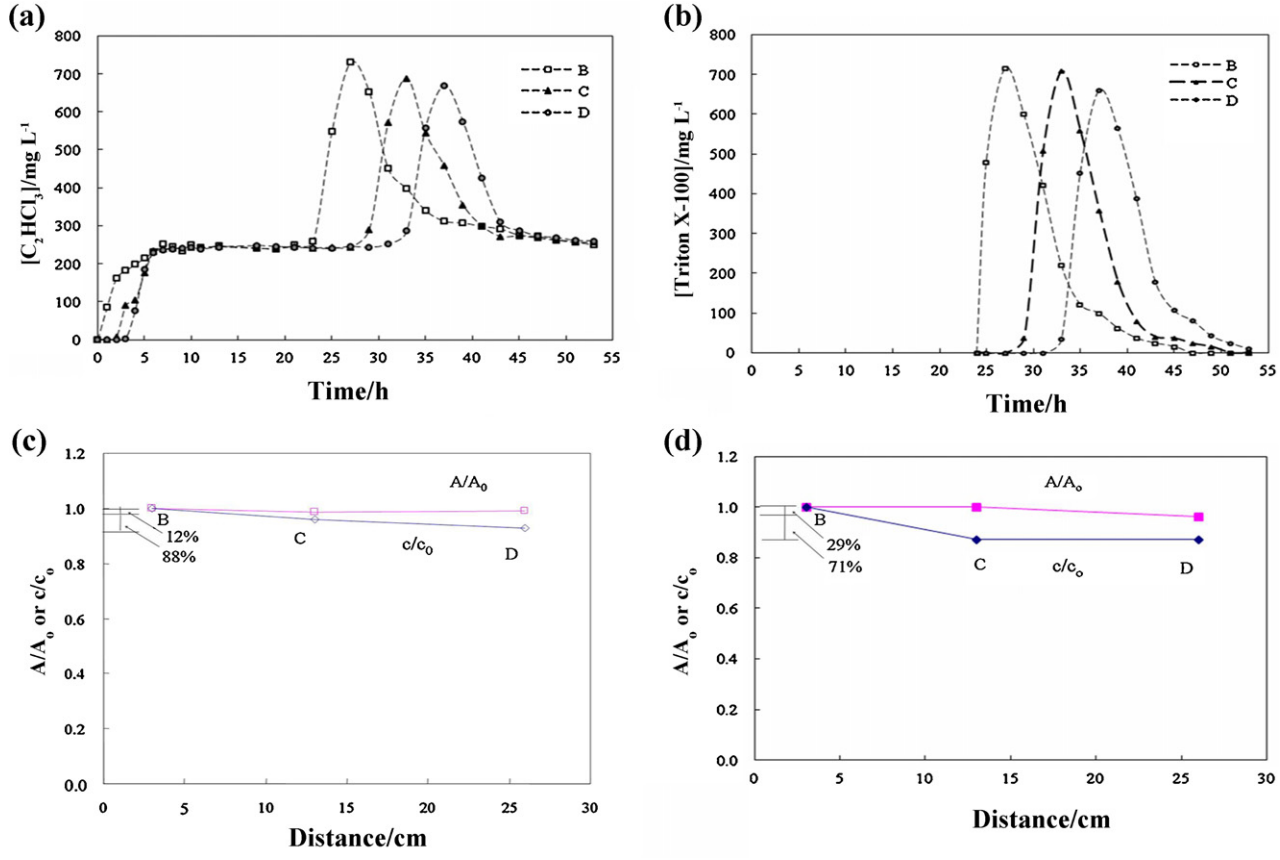

Fig. 3. Variations of (a) TCE; (b) TX100 concentrations and relationship between residual (c) TCE; (d) TX100 ratios (area under the concentration curve) versus transport distance along the tests of TX100-enhanced TCE mobility (TX100 = 1400 mg L^{-1}).

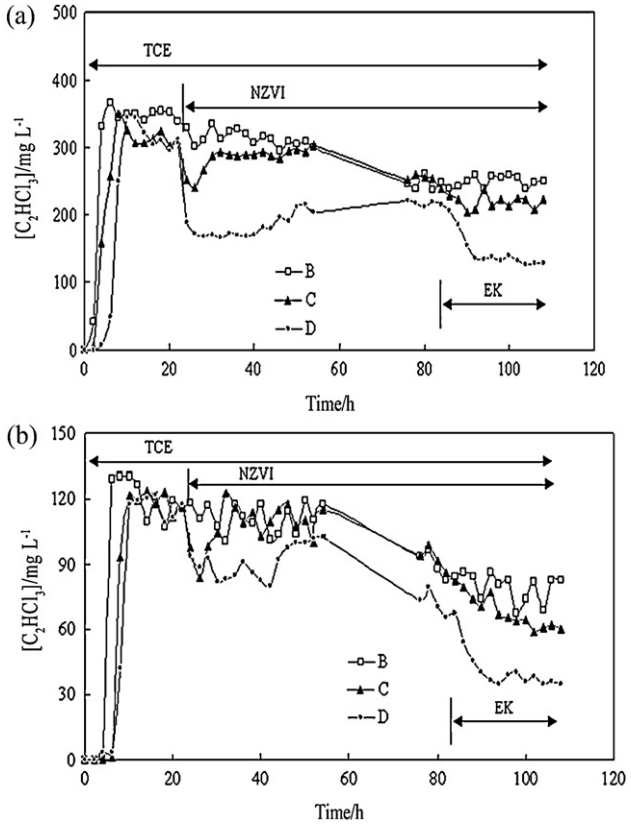

Fig. 4. Variations of TCE concentrations in (a) lower layer and (b) upper layer along the TCE degradation with NZVI and EK test.

reduction in the presence or absence of TCE was close to each other.

3.3. Degradation tests in a bench-scale sandbox

3.3.1. TCE degradation with NZVI test

As shown in Fig. 4a and b, TCE concentrations in the lower layer were higher than those in the upper layer owing to its DNAPL properties. After addition of 5 g NZVI into the PRB at the 24th hour, the residual TCE in the lower layer of point D began to decrease. To master the TCE degradation behaviors, the concentrations of TCE, Fe^{2+}, and Fe^{3+} were monitored in the lower layer of point D, located behind the PRB, as shown in Fig. 5. Concentration of TCE decreased from 300–350 to around 180 mg L^{-1} because it was reduced by NZVI resulting in the increase of Fe^{2+}, Cl-, and conductivity (EC). Before addition of NZVI, pH in the effluent chamber remained around 6.5 (Fig. 5b). As NZVI was added to the PRB, TCE in water was dechlorinated according to Eq. (1) resulting in the increase of pH because H^+ was consumed during the degradation reaction. Besides, iron hydroxide formed and precipitated on the surface of NZVI due to the raise of pH that inhibited the further TCE degradation. Therefore, TCE concentrations began to increase after 48 h of operation.

3.3.2. TCE degradation with NZVI and EK test

Continuing the TCE degradation with NZVI test, EK was applied at the 84th hour. H^+ migrated with groundwater from the anode into the NZVI PRB. H^+ not only participated in the dechlorination reaction as shown in Eq. (1), but also acid washed NZVI to clear away the precipitates on its surface to maintain activity. TCE concentrations significantly decreased from 220 to 135 mg L^{-1} starting at the 88th hour. As shown in Fig. 5b, pH raised from 7 to around 10 along the tests. EC in solution significantly increased between the 54th and 82nd hours of operation due to the addition of KCl (0.01 N) into sandbox as electrolytes for the following operation of EK. Fig. 5c shows that Cl^- concentration increases with the decrease of TCE concentration. It confirms that TCE is degraded by NZVI. Addition of NZVI and application of EK enhanced the degradation of TCE that released more Cl^- to cause the increase of EC in solution.

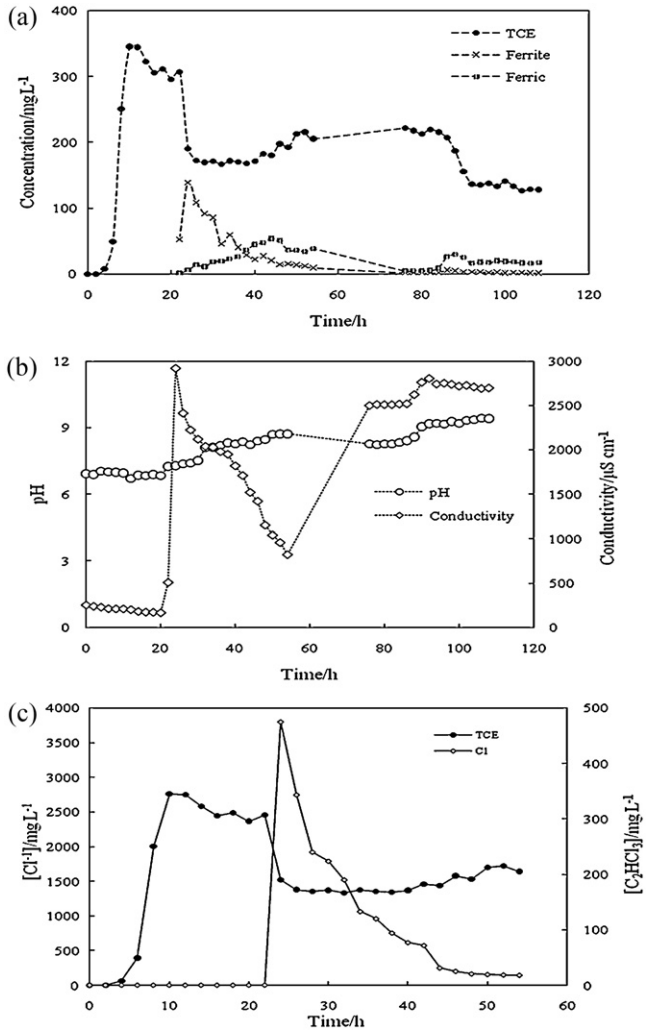

Fig. 5. Variations of (a) TCE, ferrite ion, and ferric ion; (b) pH and conductivity; (c) TCE and chloride ion for the tests of TCE degradation with NZVI reactive barrier and EK.

3.3.3. Surface morphology and characteristics of NZVI after reaction with TCE

Chain-like structure was observed for those NZVI particles not reacted with TCE (Fig. 6a), while for those NZVI reacted with TCE, their surface morphology changed and some precipitates deposited on their surface (Fig. 6b). The precipitates of rod or irregular shape may be the complexes of iron hydroxides formed by iron corrosion. Some functional groups were inspected on the surface of NZVI reacted with TCE, such as alkane, C—OH, and VC detected at 2800, 1600, and 1000 cm^{-1} (Fig. 6c) but not appeared in Fig. 6d. It showed that TCE was really dechlorinated by NZVI and EK.

4. Conclusions

This study demonstrates that NZVI PRB enhanced by EK and surfactant can effectively remove and degrade the TCE in groundwater.

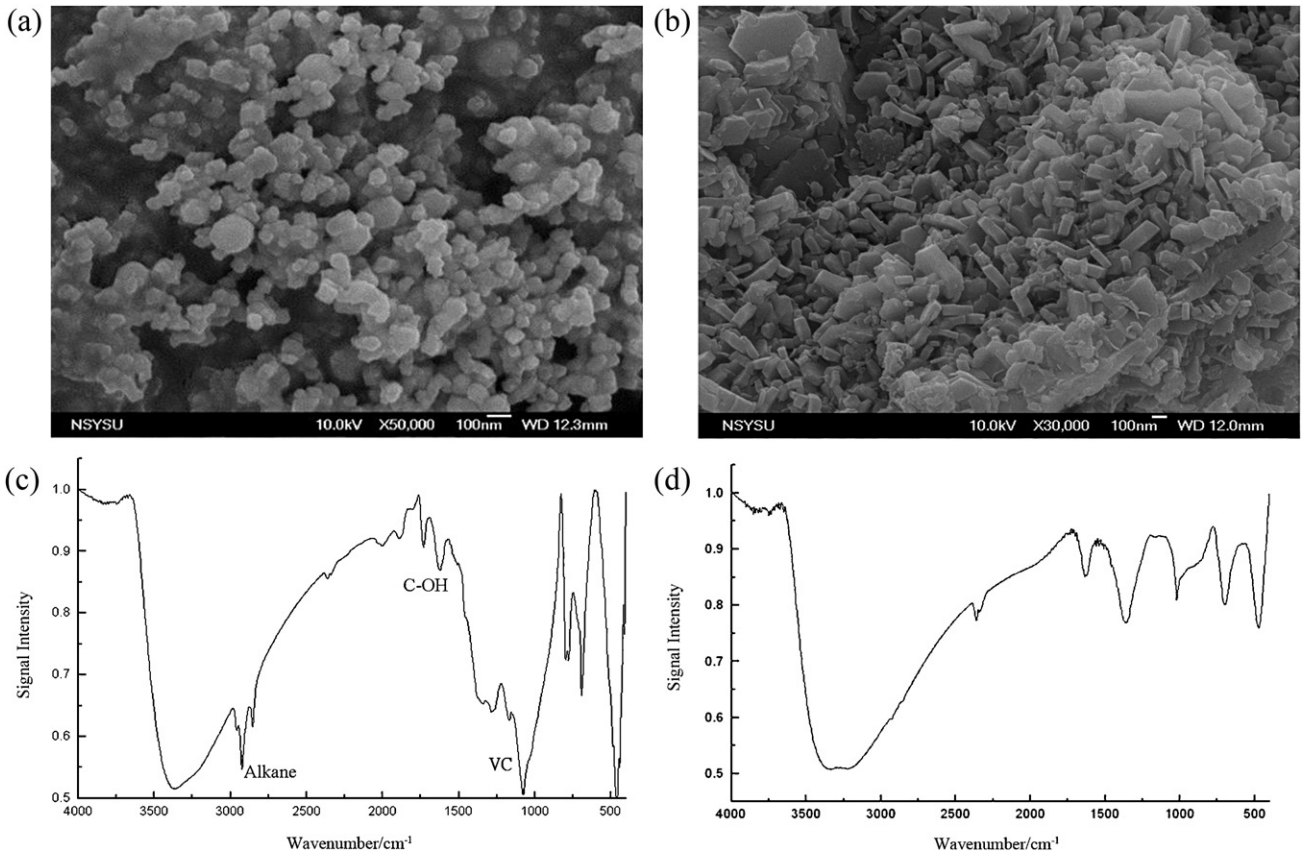

Fig. 6. Scanning electron micrographs of (a) NZVI reacted and (b) not reacted with TCE; FTIR spectra of reacted NZVI (c) in the lower layer and (d) in the upper layer of sandbox.

Surfactant raises the mobility and solubility of TCE in aquifer that increases its availability for further dechlorination of NZVI. Advection and dispersion were the main factors on reduction of TX100 while adsorption of sand had higher influences on the decrease of TCE. The concentrations of TCE in the lower layer are higher than those in the upper layer owing to its DNAPL properties. EK can promote the reactivity of NZVI by releasing H^+ near anode. H^+ not only participates in TCE dechlorination reaction but also washes away the precipitates on surface of NZVI to maintain its activity. Fe^{2+} and Cl^- were continuously produced accompanying with TCE degradation showing that TCE was dechlorinated by NZVI. Chlorinated byproducts were not detected during the lab-scale sandbox tests, i.e. TCE was completely dechlorinated by NZVI in the reactive barrier. Therefore, integration of the NZVI and EK technology can raise the remediation performance of TCE in groundwater.

Acknowledgements

The authors would like to thank National Science Council of Taiwan for financial support and the Precision Instrument Center of National Pingtung University of Science and Technology for assistance of particle characterization with BET and SEM–EDS.

References

[1] USEPA, Field Applications of In-Situ Remediation Technologies: Permeable Reactive Barriers, Office of Solid Waste and Emergency Response, Technology Innovation Office, CT, 2002.
[2] A.D. Gusmao, T.M.P. Campos, M.M.M. Nobre, E.A. Vargas Jr., J. Hazard. Mater. 110 (2004) 105.
[3] C.C. Chien, H.I. Inyang, L.G. Everett, Barrier Systems for Environmental Contaminant and Treatment, CRC/Taylor and Francis, New York, 2006.
[4] T.L. Kirschling, K.B. Gregory, E.G. Minkley Jr., Environ. Sci. Technol. 44 (2009) 3474.
[5] S.S. Chen, Y.C. Huang, T.Z. Kuo, Ground Water Monit. Remediat. 30 (2010) 90.
[6] C. Silvia, D.M. Antonio, S. Rajandrea, Water Air Soil Pollut. 215 (2011) 595.
[7] L.J. Matheson, P.G. Tratnyek, Environ. Sci. Technol. 28 (1994) 2045.
[8] A.L. Roberts, L.A. Totten, W.A. Arnold, D.R. Burris, T.J. Campbell, Environ. Sci. Technol. 30 (1996) 2654.
[9] J. Farrell, N. Melitas, M. Kason, T. Li, Environ. Sci. Technol. 34 (2000) 2549.
[10] J.L. Chen, S.R. Al-Abed, J.A. Ryan, Z. Li, J. Hazard. Mater. 83 (2001) 243.
[11] G.A. Loraine, Water Res. 35 (2001) 1453.
[12] C.J. Clark II, P.S.C. Rao, M.D. Annable, J. Hazard. Mater. 96 (2003) 65.
[13] W.X. Zhang, C.B. Wang, H.L. Lien, Catal. Today 40 (1998) 387.
[14] J.H. Chang, S.F. Cheng, J. Hazard. Mater. 131 (2006) 153.
[15] M.C. Shin, H.D. Chio, D.H. Kim, K. Baek, Desalination 223 (2008) 299.
[16] R.W. Gillham, S.F. O'Hannesin, Ground Water 32 (1994) 958.
[17] W.A. Arnold, A.L. Roberts, Environ. Sci. Technol. 34 (2000) 1794.
[18] C.B. Wang, W.X. Zhang, Environ. Sci. Technol. 31 (1997) 2154.
[19] S.Y. Choe, Y. Chang, K.Y. Hwang, J. Khim, Chemosphere 41 (2000) 1307.
[20] H.L. Lien, W.X. Zhang, Colloids Surf. A 191 (2001) 97.
[21] T. Masciangioli, W.X. Zhang, Environ. Sci. Technol. 37 (2003) 102.
[22] W.X. Zhang, J. Nanopart. Res. 5 (2003) 323.
[23] A.P. Shapiro, P.C. Renaud, R.F. Probstein, Phys. Chem. Hydrodyn. 11 (1989) 785.
[24] J. Wan, Z. Li, X. Lu, J. Hazard. Mater. 184 (2010) 184.
[25] E.H. Jones, D.A. Reynolds, A.L. Wood, Ground Water 49 (2011) 172.
[26] K.R. Reddy, D.K. Kenneth, C. Claudio, Sep. Purif. Technol. 79 (2011) 230.
[27] G.C.C. Yang, Y.I. Chang, Sep. Purif. Technol. 79 (2011) 278.
[28] K.R. Reddy, C. Cameselle, Electrochemical Remediation Technologies for Polluted Soils, Sediments and Groundwater, Wiley, New York, 2009.
[29] K. Maturi, K.R. Reddy, C. Cameselle, Sep. Sci. Technol. 44 (2009) 2385.
[30] K.R. Reddy, C. Cameselle, P.R. Ala, J. Appl. Electrochem. 40 (2010) 1269.
[31] D.A. Sabatini, R.C. Knox, J.H. Harwell, B. Wu, J. Contam. Hydrol. 45 (2000) 99.
[32] C. St-Pierre, R. Martel, U. Gabriel, R. Lefebvre, T. Robert, J. Hawari, J. Contam. Hydrol. 71 (2004) 155.
[33] Z. Li, H. Hanlie, Water Res. 42 (2008) 605.
[34] T.T. Tsai, C.M. Kao, T.Y. Yeh, S.H. Liang, H.Y. Chien, J. Hazard. Mater. 161 (2009) 111.

[35] Y.C. Lee, C.W. Kim, J.Y. Lee, Desalination Water Treat. 10 (2009) 33.
[36] S. Harendra, C. Vipulanandan, Ind. Eng. Chem. Res. 50 (2011) 5831.
[37] M.C. Shin, J.S. Yang, G.Y. Park, Korean J. Chem. Eng. 28 (2011) 1047.
[38] M. Zhang, F. He, D. Zhao, X. Hao, Water Res. 45 (2011) 2401.
[39] Y.C. Huang, S.Y. Huang, J. Chin. Inst. Environ. Eng. 16 (2006) 151.
[40] S.Y. Huang, Surfactant-enhanced permanganate oxidation of trichloroethylene from groundwater, Thesis, National Pingtung University of Science and Technology, Taiwan, 2004.
[41] G. Tchobanoglous, F.L. Burton, H.D. Stensel, Wastewater Engineering Treatment and Reuse, 4th ed., Mecalf & Eddy/McGraw Hill, New York, 2002 (Chapter 4).